Cellular Physiology and Biochemistry
Cell Physiol Biochem 2016;39:1209-1228
DOI: 10.1159/000447827
Published online: September 05, 2016
Accepted: August 03, 2016

Original Paper

Expression of JAK3 Sensitive Na^+ Coupled Glucose Carrier SGLT1 in Activated Cytotoxic T Lymphocytes

Shefalee K. Bhavsar[a] Yogesh Singh[a] Piyush Sharma[b] Vishal Khairnar[b] Zohreh Hosseinzadeh[a,f] Shaqiu Zhang[a] Monica Palmada[g] Ivan Sabolic[c] Hermann Koepsell[d] Karl S. Lang[b] Philipp A. Lang[e] Florian Lang[a,e]

[a]Department of Cardiology, Vascular Medicine and Physiology, University of Tuebingen, [b]Department of Immunology, University of Essen, Essen, Germany; [c]Molecular Toxicology Unit, Institute for Medical Research and Occupational Health, Zagreb, Croatia; [d]Department of Molecular Plant Physiology and Biophysics, Julius-von Sachs Institute, University of Würzburg, Würzburg, [e]Department of Molecular Medicine II, Heinrich Heine University Düsseldorf, Düsseldorf, [f]Experimental Retinal Prosthetics Group, Centre for Ophthalmology, Institute for Ophthalmic Research, Tuebigen, [g]Faculty of Life Sciences, Rhein Waal University of Applied Sciences, Kleve, Germany

Key Words
Cytotoxic T lymphocytes • Glucose uptake • Jurkat T cells • Energy depletion • Janus kinase • Tumor cells

Abstract
Background: Similar to tumor cells, activated T-lymphocytes generate ATP mainly by glycolytic degradation of glucose. Lymphocyte glucose uptake involves non-concentrative glucose carriers of the GLUT family. In contrast to GLUT isoforms, Na^+-coupled glucose-carrier SGLT1 accumulates glucose against glucose gradients and is effective at low extracellular glucose concentrations. The present study explored expression and regulation of SGLT1 in activated murine splenic cytotoxic T cells (CTLs) and human Jurkat T cells. ***Methods:*** FACS analysis, immunofluorescence, confocal microscopy, chemiluminescence and Western blotting were employed to estimate SGLT1 expression, function and regulation in lymphocytes, as well as dual electrode voltage clamp in SGLT1 ± JAK3 expressing *Xenopus* oocytes to quantify the effect of janus kinase3 (JAK3) on SGLT1 function. ***Results:*** SGLT1 is expressed in murine CTLs and also in human Jurkat T cells. 2-(N-(7-nitrobenz-2-oxa-1,3-diazol-4-yl)amino)-2-deoxyglucose uptake was significantly decreased by SGLT1-blocker phloridzin (0.2 mM) and by pharmacological inhibition of JAK3 with WHI-P131 (156 μM), WHI-P154 (11.2 μM) and JAK3 inhibitor VI (0.5 μM). Electrogenic glucose transport ($I_{glucose}$) in *Xenopus* oocytes expressing human SGLT1 was increased by additional expression of human wild type JAK3, active ^{A568V}JAK3 but not inactive ^{K851A}JAK3. Coexpression of JAK3 enhanced the maximal transport rate without significantly modifying affinity of the carrier. $I_{glucose}$ in SGLT1+JAK3 expressing oocytes was significantly decreased by WHI-P154 (11.2 μM). JAK3 increased the SGLT1 protein abundance in the cell membrane. Inhibition of carrier insertion by brefeldin A (5 μM) in SGLT1+JAK3 expressing oocytes resulted in a decline of $I_{glucose}$, which was

Prof. Dr. Florian Lang
Department of Physiology, University of Tuebingen, Gmelinstr. 5, D-72076 Tuebingen (Germany)
Tel. +49 7071/2972194, Fax +49 7071/295618, E-Mail florian.lang@uni-tuebingen.de

similar in presence and absence of JAK3. ***Conclusions:*** SGLT1 is expressed in murine cytotoxic T cells and human Jurkat T cells and significantly contributes to glucose uptake in those cells post activation. JAK3 up-regulates SGLT1 activity by increasing the carrier protein abundance in the cell membrane, an effect enforcing cellular glucose uptake into activated lymphocytes and thus contributing to the immune response.

Introduction

The tyrosine kinase, janus kinase 3 (JAK3) contributes to the signaling of hematopoietic cell cytokine receptors [1-5]. In lymphocytes and tumor cells JAK3 fosters cell proliferation and counteracts apoptosis [6-8]. Accordingly, JAK3 inhibitors stimulate apoptosis of tumor cells [9, 10]. In contrast, JAK3 fosters apoptosis of dendritic cells [11]. JAK3 has been implicated in the response to hypoxia and ischemia-reperfusion [12-14].

The gain of function mutation of ^{A572V}JAK3 [15] has been found in acute megakaryoplastic leukemia [16, 17]. Replacement of the ATP coordinating lysine by alanine in the catalytic subunit results in the inactive ^{K855A}JAK3 [15].

Cellular functions regulated by JAK3 include glucose metabolism [12]. The isoform JAK2 has previously been shown to up-regulate the Na^+ coupled glucose carrier SGLT1 [18], which mediates secondary active transport driven by the electrochemical Na^+ gradient [19]. SGLT1 and its isoform SGLT2 are expressed in epithelial cells and accomplish the concentrative cellular uptake of glucose from the intestinal or renal tubular lumen across the apical cell membrane [19]. SGLT1 is further expressed in a wide variety of tumor cells [20-27]. Tumor cells meet their need for energy mainly by glycolysis [22, 28-31]. In tumor tissue, the excessive cellular glucose uptake may result in a sharp decrease of extracellular glucose concentrations requiring concentrative cellular uptake for the maintenance of adequate intracellular glucose concentrations. Unlike the facilitative glucose carriers the Na^+-coupled glucose carriers could transport against a chemical gradient and allow cellular glucose accumulation even at low extracellular glucose concentrations [19].

Mechanisms upregulating SGLT1 expression and activity in tumor cells involve EGF receptor dependent stabilization of SGLT1 [21, 27] and stimulation of SGLT1 by JAK2 [18]. Moreover, SGLT1 is upregulated by the HPV18 E6 protein from human papilloma virus [32], the causative agent of cervical cancer, other anogenital cancers and a subset of head and neck carcinomas [33-35].

Similar to tumor cells, activated T lymphocytes [36] and other monocytes depend on glycolysis for ATP production during infection. Following activation T cells switch from oxidative phosphorylation prevailing in naive cells to glycolysis thus providing oxygen-independent ATP production [36]. Effector CTLs may have to migrate, survive and produce effector cytokines in the hypoxic environment of inflammatory tissue. Moreover, lymphoid tissue is also relatively hypoxic with oxygen tension ranging from 1 to 5% [37]. A switch to glycolysis may thus allow CTLs to proliferate and mediate their effector function in relatively hypoxic conditions [38]. Effector T cells (Teff) are particularly dependent on glycolysis, while regulatory T cells (Tregs) generate ATP in large part by lipid oxidation [39]. Lymphocyte glycolysis is stimulated by activation of the Interleukin 7 receptor [40], which may activate JAK3 [31]. Besides its role in energy supply, glycolysis may provide a source of carbon for the synthesis of nucleic acids and phospholipids [41]. The dependence of CTLs on glycolysis renders those cells dependent on efficient glucose uptake for survival and function [42, 43].

Similar to T lymphocytes, B lymphocytes [44], macrophages [45-47] and mast cells [40] may generate ATP in large part by glycolysis.

At least in theory, facilitative glucose uptake may become insufficient in tissues with low extracellular glucose concentration. The present study thus explored whether SGLT1 is expressed in activated T lymphocytes from mice and in human Jurkat T cells and whether SGLT1 contributes to glucose uptake by those cells. Moreover, the present study explored

whether SGLT1 is regulated by JAK3.

To this end cytotoxic T cells cultured from wild type mice were activated with anti-CD3 for 48h and later cultured in IL2 supplemented medium to generate mature cytotoxic T cell blasts. SGLT1 expression was analysed by FACS analysis, confocal microscopy and Western blotting. Moreover, glucose uptake was determined in the absence and presence of SGLT1 inhibitor phloridzin and JAK3 inhibitors WHI-P131, WHI-P154 and JAK3 inhibitor VI. In an additional series of experiments, the influence of JAK3 on SGLT1 activity was determined in *Xenopus laevis* oocytes. SGLT1 was expressed in *Xenopus* oocytes with or without wild type JAK3, active ^{A568V}JAK3 or inactive ^{K851A}JAK3 and SGLT1 protein abundance in the cell membrane determined by chemiluminescence as well as electrogenic glucose transport utilizing dual electrode voltage clamp.

Materials and Methods

Culture of Jurkat T cells and Caco2 cells

Human Jurkat T cells [48] were cultured in RPMI 1640 supplemented with 10% FBS, 1% penicillin/streptomycin, HEPES, L-glutamine, sodium-pyruvate, NEAA- non-essential amino acids and ß-mercaptoethanol at 37°C in a humidified atmosphere with 5% CO_2 / air.

Caco2 cells were cultured in DMEM medium containing 4.5 g/L glucose, 20% FBS, 1% L-glutamine, 1% non-essential amino acids and 1% penicillin/streptomycin. The cells were grown on 12-mm glass coverslips (neoLab Migge Laborbedarf-Vertriebs GmbH, Heidelberg, Germany) in 12-well plates (5×10^4 cells/well/coverslip). Two days after plating, the cells reached 80–90% confluence and were used as positive control for confocal staining of SGLT1.

Splenic CD8⁺ cytotoxic T-lymphocyte culture from mice

All animal experiments were conducted according to German law and approved by the respective authority. Spleens were isolated from B6129SF2/J male and female wildtype mice as well as from SGLT1 knockout mice [49].

Cytotoxic T lymphocytes (CTL) were cultured from the splenic T-cells as described earlier [50]. For activation of primary naive T cells, spleens from wildtype mice were disaggregated following red blood cell lysis. Cells were cultured in RPMI-1640 medium containing 50 mM L-glutamine, 10% heat-inactivated FBS, 50 µM β-mercaptoethanol and 1% penicillin-streptomycin. Single-cell suspensions from splenocytes adjusted to a density of 5×10^6 cells/mL were stimulated with monoclonal anti-CD3 (5 µg/mL; 145-2C11, R and D Systems) to 'trigger' the T-cell receptor (TCR). For generation of mature cytotoxic T-lymphoblasts, mouse T cells grown from spleen preparations cultured for 48 h in the presence of stimulus (monoclonal antibody 2C11) were washed and resuspended at a density of 4×10^5 cells per mL with IL-2 (0.02 µg/mL; 360 IU/mL) for 72 h to generate mature CTL blasts. After activation and clonal expansion mature cytotoxic T-cell blasts were characterized phenotypically by flow cytometry. As a result, more than 80% of the cells were positive for CD8⁺. Cells were further maintained in medium containing IL-2 (0.02 µg/mL; 360 IU/mL). Cells were counted each day, and maintained to the optimum cell density with IL-2 supplementation in the medium.

Flow cytometric analysis and phenotyping of the cells

Mature cytotoxic T-cell blasts were analysed with the standard multicolor flow cytometry settings and commercially available specific fluorescence conjugated antibodies as follows: Fluorescein isothiocyanate (FITC) or Phycoerythrin (PE) conjugated anti-CD4, Allophycocyanin (APC) or Cyanine 5.5 (Cy5.5) conjugated anti-CD8, PE conjugated anti-CD25, PE conjugated anti-CD62L, APC conjugated anti-CD25, PE conjugated anti-CD98, PE-anti-CD71 and APC anti-TCRbeta (BD Biosciences, Heidelberg, Germany). A minimum of $2x10^5$ cells were washed and stained for 30 min at 4°C with saturating concentrations of antibody in RPMI-1640 medium and 0.5% FBS. Cells were washed and resuspended in RPMI-1640 medium and 0.5% FBS before being acquired on a FACS Calibur (BD, Heidelberg, Germany). A minimum of 5×10^4 relevant events were measured and stored ungated. Live cells (>90% of total acquired events) were gated according to their forward scatter and side scatter. Data was analyzed using Cell Quest Pro software (BD Biosciences, Heidelberg, Germany).

SGLT1 flow cytometry

Cell surface expression of SGLT1 was determined using specific antibodies for human (Millipore, Billerica, MA, USA) and murine SGLT1 described earlier [49]. A minimum of $2x10^5$ cells were washed with PBS and stained with primary anti-SGLT1 antibody for at least 6 h followed by washing twice with ice-cold PBS and staining with corresponding secondary goat anti-rabbit FITC conjugated antibody (1:500, Invitrogen, Darmstadt, Germany) for 1 h. After washing with PBS cells were analyzed by flow cytometry. FITC fluorescence intensity was measured in FL-1 fluorescence channel on a FACS calibur (BD, Heidelberg, Germany). A minimum of 5×10^4 relevant events were collected and stored ungated. Live cells (>90% of total acquired events) were gated according to their forward scatter and side scatter. Data were analyzed using Cell Quest Pro software (BD Biosciences, Heidelberg, Germany). To determine expression on specific $CD8^+/CD4^+$ cell subsets in murine CTLs, cells were stained in addition with PE-conjugated anti-CD4 antibody and APC-conjugated anti-CD8 antibody (BD Biosciences, Heidelberg, Germany). The fluorescence was measured by standard multicolor flow cytometry settings. PE fluorescence measured in FL-2 and APC fluorescence measured in FL-4 channel together with FITC fluorescence measured in channel FL-1.

SGLT1 mRNA expression

Total RNA was isolated from total CTLs, purified $CD4^+$ T cells and purified $CD8^+$ T cells activated for 48 hours in presence of IL-2 (0.02 µg/mL; 360 IU/mL) and anti-CD3 (5 µg/mL) by mRNAeasy isolation kit (QIAGEN, Germany) according to manufacturer's instructions and 1 µg RNA was converted into cDNA using Superscript III reverse transcriptase cDNA synthesis kit (Invitrogen, Germany). RT-PCR reaction was set up using 10 ng cDNA using 2x KAPA-SYBR Green (Peqlab, Germany) and forward as well as reverse primers for SGLT1 expression. Real-time quantitative RT-PCR analysis was performed using BioRad CFX96 Real-Time thermal cycler (BioRad, USA). The relative expression level of miRNAs was normalized to that of internal control GAPDH by using the $2^{-\Delta\Delta Ct}$ cycle threshold method as described previously [51].

The following primers were used:
SGLT-1-F 5'- TGCACCTGTACCGTTTGTGT-3'
SGLT-1-R 5'- GGGGGCTTCTGTGTCTATTT-3',
GAPDH-F 5'-TCTGACCACAGTGAGGAATGTCCAC-3'
GAPDH-R 5'-TTGATGGCAACAATCTCCAC-3'

Cellular glucose uptake

The fluorescent glucose analogue 2-(N-(7-nitrobenz-2-oxa-1,3-diazol-4-yl)amino)-2-deoxyglucose (2-NBD-glucose; Invitrogen, Darmstadt, Germany) was used to measure the relative uptake of glucose by flow cytometry. In each condition, cells (1×10^6) were incubated with 2-NBD-glucose (30 µM) in phosphate buffered saline for 1 hour at 37°C, subsequently washed twice in cold PBS and analyzed by flow cytometry in fluorescence channel FL1. Changes in glucose uptake after inhibitor treatment were calculated as differences in geometric mean of the fluorescence. Flow cytometry settings were made by standard protocols relative to the unstained cells.

To determine the effect of phloridzin on total glucose uptake by CTLs and Jurkat T cells, cells (1×10^6) were incubated with the indicated concentrations of phloridzin (Sigma Aldrich, Taufkirchen München, Germany) in cell culture medium for the indicated time periods. Following incubation cells were washed and glucose uptake measured as described above in the continuous presence or absence of phloridzin. In some experiments phloridzin was added only in the 2-NDB-glucose uptake solution without any pre-incubation with the inhibitor.

To determine the effect of JAK3 inhibition on glucose uptake, cells (1×10^6) were treated for 12 h with the JAK3 inhibitors WHI-P131/JANEX-1 (4-(4'-Hydroxyphenyl)amino-6,7-dimethoxyquinazoline, 156 µM), WHI-P154 (4-[(3'-Bromo-4'-hydroxyphenyl)amino]-6,7-dimethoxyquinazoline, 11.2 µM) or JAK3 Inhibitor VI (0.5 µM) (Calbiochem, Merck KGaA, Darmstadt, Germany). At the end of the incubation period cells were washed with PBS and glucose uptake determined as described above. For each condition untreated cells were used as control.

Immunostaining and confocal microscopy

SGLT1 protein abundance was determined by immunofluorescence. The cells ($1x\ 10^6$) were washed with PBS and fixed for 20 min in 4% paraformaldehyde in PBS/0.1% Triton. The cells were washed again and then blocked in 5% goat serum in PBS/0.1% Triton for 1 hour at room temperature. To detect the expression of SGLT1 the cells were incubated overnight at 4°C with specific antibodies for human (Millipore,

Billerica, MA, USA) and murine rabbit anti-SGLT1 described earlier [49]. After incubation, the cells were rinsed three times with PBS/0.1% Triton and incubated with the secondary FITC anti-rabbit antibody (1:500, Invitrogen, Darmstadt, Germany) for 1 h at room temperature. After washing with PBS/0.1% Triton the nuclei were stained with DRAQ-5 dye (1:1000, Biostatus, Leicestershire, UK) for 5 min at 37°C. The slides were mounted with Prolong antifade reagent (Invitrogen, Darmstadt, Germany). The images were taken on a Zeiss LSM 5 *EXCITER* Confocal Laser Scanning Microscope, equipped with a 405–633 nm laser (Carl Zeiss MicroImaging GmbH, Germany) using a water immersion Plan-Neofluar 63/1.3 NA DIC. Three independent experiments were performed for each set of experiments.

Western blotting

The cells were lysed in cell lysis buffer (50 mM Tris-HCl, pH 7.5, 150 mM NaCl, 1% Triton X-100, 0.5% SDS, 1 mM NaF, 1 mM Na3VO4, 0.4% ß-mercaptoethanol) containing protease inhibitor cocktail (Sigma). 100-50 µg of protein were solubilized in Laemmli sample buffer at 95°C for 5 min and resolved by 10% SDS-PAGE. For immunoblotting proteins were electro-transferred onto a nitrocellulose membrane and blocked with 5% nonfat milk in TBS-0.10% Tween 20 (TBST) at room temperature for 1 hour. Then, the membrane was incubated with affinity purified anti-SGLT1 antibody (1:1000, rabbit polyclonal antibody, Millipore, Billerica, MA, USA) or with murine rabbit anti-SGLT1 at 4°C overnight. After washing 3 times with TBST (10 min each) the blots were incubated with horseradish peroxidase conjugated secondary anti-rabbit antibody (1:2000; Cell Signaling Technology, MA, USA) for 1 hour at room temperature. After washing antibody binding was detected with the ECL detection reagent (Cell Signaling Technology, MA, USA). For loading control the same membranes were stripped with stripping buffer (Millipore, Billerica, MA, USA) and reblotted with rabbit anti-α/β-Tubulin antibody (1:1000; Cell Signaling Technology, MA, USA). Antibody-binding was quantified with Quantity One Software (Biorad, Germany).

Constructs

For generation of cRNA, constructs were used encoding wild-type human SGLT1 (SLC5A1) and wild-type murine JAK3 (Imagenes, Berlin, Germany) [52, 53]. Further, an inactive ^{K851A}JAK3 mutant, corresponding to human ^{K855A}JAK3 mutant [15] and the active ^{A568V}JAK3 mutant, corresponding to human ^{A572V}JAK3 mutant [15] were generated by site-directed mutagenesis (QuikChange II XL Site-Directed Mutagenesis Kit; Stratagene, Heidelberg, Germany) according to the manufacturer's instructions [54]. The following primers were used:

^{A568V}JAK3:5′ GAGTCTTTTCTGGAAGTCGCAAGCTTGATGAGC 3′;

^{A568V}JAK3: 5′ GCTCATCAAGCTTGCGACTTCCAGAAAAGACTC 3′

^{K851A}JAK3: 5′ CCCCTGGTGGCAGTGGCACAGCTACAGCACAGC 3′and

^{K851A}JAK3: 5′GCTGTGCTGTAGCTGTGCCACTGCCACCAGGGG 3′.

Underlined bases indicate mutation sites. The mutants were sequenced to verify the presence of the desired mutation. The mutants were used for generation of cRNA as described previously [55-57].

Voltage clamp in Xenopus oocytes

Xenopus oocytes were prepared as previously described [58-60]. 10 ng of wild type JAK3 cRNA were injected on the first day and 10 ng SGLT1 cRNA on the same day after preparation of the oocytes. The oocytes were maintained at 17°C in ND96 solution containing (in mM): 96 NaCl, 4 KCl, 1.8 $MgCl_2$, 0.1 $CaCl_2$, 5 HEPES, pH 7.4, supplemented with theophyllin (90 mg/L), gentamycin (100 mg/L), tetracyclin (50 mg/L) and ciprofloxacin (1.6 mg/L). The final solutions were titrated to pH 7.4 using NaOH. Where indicated, WHI-P154 (4-[(3′-Bromo-4′-hydroxyphenyl)amino]-6,7-dimethoxyquinazoline, 11.2 µM), actinomycin D (10 µM) or brefeldin A (5 µM) were added. The voltage clamp experiments [61-63] were performed at room temperature 3 days after injection. Two-electrode voltage-clamp recordings were performed at a holding potential of -70 mV. The data were filtered at 10 Hz and recorded with a Digidata A/D-D/A converter and Clampex V.9 software for data acquisition and analysis (Axon Instruments)[64-66]. The control superfusate (ND96) contained 96 mM NaCl, 2 mM KCl, 1.8 mM $CaCl_2$, 1 mM $MgCl_2$ and 5 mM HEPES, pH 7.4. Glucose was added to the solutions at a concentration of 10 mM unless otherwise stated. The flow rate of the superfusion was approx. 20 mL/min, and a complete exchange of the bath solution was reached within about 10 s [67-69].

Detection of SGLT1 cell surface expression by chemiluminescence

Defolliculated oocytes were incubated with rabbit polyclonal anti-SGLT1 antibody (1:200) and subsequently with secondary, HRP-conjugated goat anti-rabbit antibody (1:1500, Cell Signaling Technology,

MA, USA). Post-staining individual oocytes were placed in 96 well plates with 20 µl of SuperSignal ELISA Femto Maximum Sensitivity Substrate (Pierce, Rockford, IL, USA) and chemiluminescence of single oocytes was quantified in a luminometer (Walter Wallac 2 plate reader, Perkin Elmer, Juegesheim, Germany) by integrating the signal over a period of 1 s. Results display normalized relative light units [70, 71].

Statistical analysis

Data are provided as means ± SEM, n represents the number of oocytes and mice investigated. All experiments were repeated with at least 3 batches of oocytes; in all repetitions qualitatively similar data were obtained. As expression of SGLT1 and/or JAK3 may vary from batch to batch of oocytes, comparisons were always made within the same oocyte batch. Data were tested for significance using ANOVA or t-test, as appropriate. Results with $p<0.05$ were considered statistically significant.

Results

Expression of SGLT1 and phloridzin sensitive glucose uptake in activated murine cytotoxic T lymphocytes

SGLT1 expression in murine cytotoxic T lymphocytes was detected with immunofluorescence and confocal microscopy. As shown in Fig.1A, SGLT1 is mainly localized in the cell membrane. Control staining with secondary antibody alone did not result in any significant fluorescence signal (not shown). Similarly, no staining was observed in CTLs

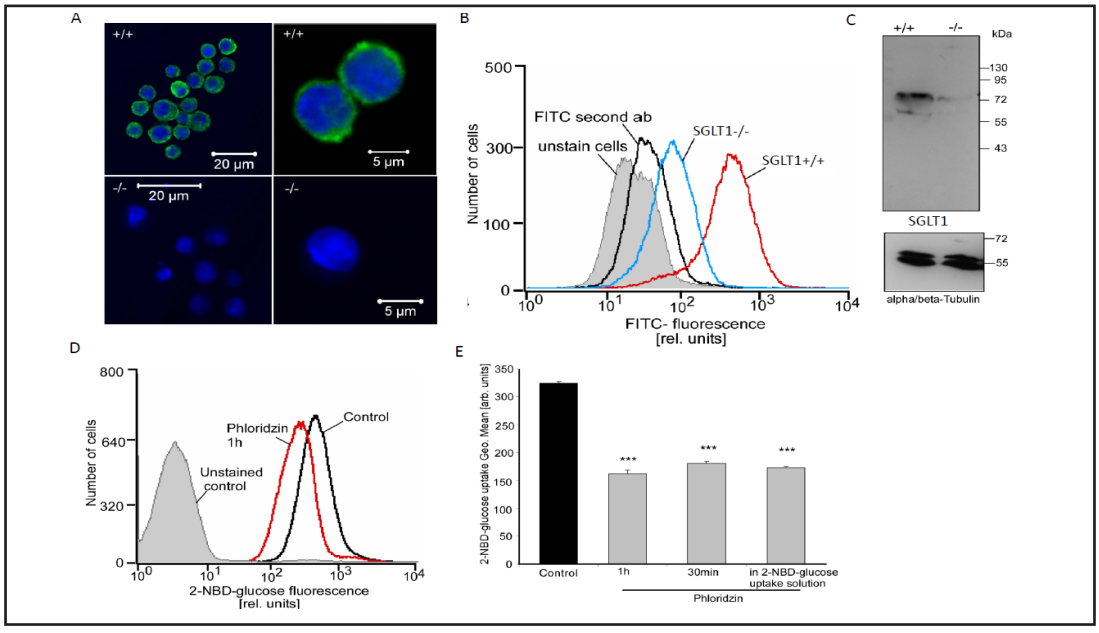

Fig. 1. SGLT1 expression and phloridzin-sensitive glucose uptake in activated murine cytotoxic T lymphocytes. A: Confocal microscopy of SGLT1 protein expression in cytotoxic mature T cell blasts (CTL) isolated from wild type (upper panels) and SGLT1 knockout (lower panels) mice. The CTLs were subjected to immunofluorescent staining using rabbit anti-murine SGLT1 antibody visualized by staining with anti-rabbit FITC-conjugated secondary antibody (green). DRAQ-5 dye (blue) was used for nuclear staining. B: Original histograms of the SGLT1 staining in murine cytotoxic T cells (CTL). Histograms represent unstained wild type cells (grey filled), wild type cells stained with secondary FITC antibody alone (black line), as well as wild type cells (red line) and SGLT1 knockout cells (blue line) stained with SGLT1 antibody followed by secondary FITC antibody. C: Original Western blots showing expression of SGLT1 in murine CTLs. D: Original histograms of 2-NBD-glucose uptake in CTLs without (black line) or with 1 hour incubation with phloridzin (red line). Grey filled histogram shows unstained cells. E: Arithmetic means ± SEM (n = 4) of geometric means for the 2-NBD- glucose uptake into CTL in the absence (black bar) and presence (grey bars) of phloridzin (0.2 mM) added for the indicated time periods. *** ($p<0.001$) indicates statistically significant difference from the absence of phloridzin in 2-NBD-glucose uptake.

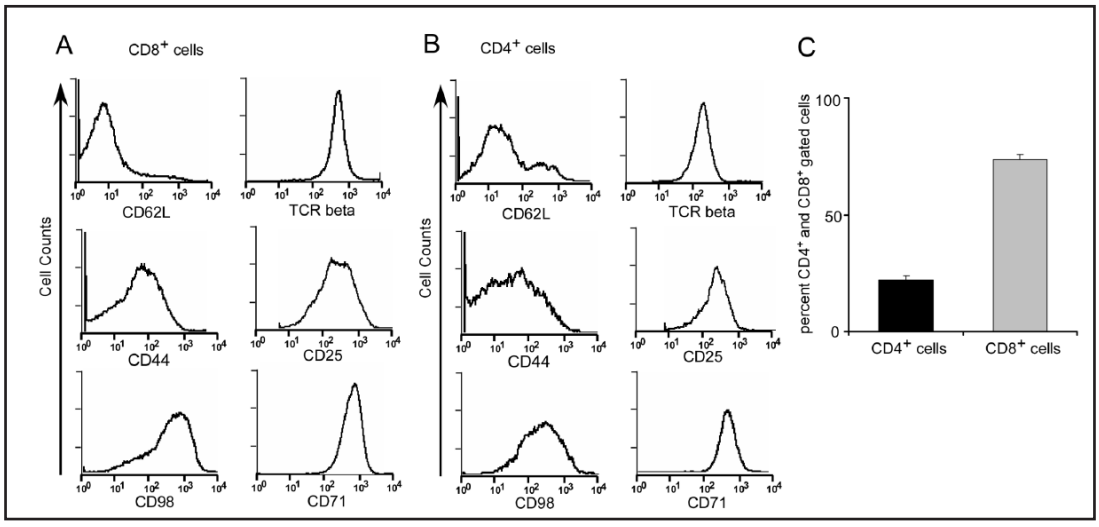

Fig. 2. Phenotype of mature CTL blasts. Mature cytotoxic T cell blasts were analysed with the standard multicolor flow cytometry settings and commercially available (BD Biosciences) specific fluorescence conjugated antibodies - Fluorescein isothiocyanate (FITC) or Phycoerythrin (PE) conjugated anti-CD4, Allophycocyanin (APC) or Cyanine 5.5 (Cy5.5) conjugated anti-CD8, PE conjugated anti-CD25, PE conjugated anti-CD62L, APC conjugated anti-CD25, PE conjugated anti-CD98, PE-anti-CD71 and APC anti-TCRbeta. Live cells (>90% of total acquired events) were gated according to their forward scatter and side scatter. The cells were again gated for CD8 and CD4 positive cells and respective fluorescence calculated for cells in CD8 and CD4 gate. Data was analyzed using Cell Quest Pro software (BD Biosciences, Heidelberg, Germany). A: Phenotype of $CD8^+$ T cells B: Phenotype of $CD4^+$ T cells C: Percent $CD4^+$ and $CD8^+$ T cells in the CTL cultures used for experiments.

isolated from SGLT1 knockout mice (Fig.1A). In a second series of experiments, SGLT1 protein abundance at the surface of CTL was measured by FACS analysis. As illustrated in Fig. 1B, SGLT1 is observed in CTL from wild type mice. The fluorescence was approximately one order of magnitude lower in CTL from SGLT1 knockout mice. Staining with secondary antibody resulted in a similarly faint staining. Taken together, the experiments demonstrate expression of SGLT1 in murine CTLs. SGLT1 was further detected by Western blotting in wildtype mice. Again, no clear band was seen in CTLs from SGLT1 knockout mice. The loading control α/β-Tubulin was similarly expressed in both genotypes (Fig.1C). Hence, SGLT1 is expressed in activated murine CTLs.

In order to determine the contribution of SGLT1 to glucose uptake by CTLs, glucose uptake into CTLs was determined in the absence and presence of SGLT1 inhibitor phloridzin. As shown in Fig.1D, incubation with phloridzin resulted in a significant reduction of glucose uptake into CTLs. Similar results were obtained in CTL pretreated for 30 min, 1 h or 2 h as in CTLs exposed to phloridzin without preincubation (Fig. 1E).

Additional experiments were performed to discriminate between $CD4^+$ and $CD8^+$ T cells. The phenotype of mature CTLs was determined by FACS analysis (Fig. 2). SGLT1 was expressed in both, $CD4^+$ and $CD8^+$ T cells (Fig. 3). Accordingly, in both, $CD4^+$ and $CD8^+$ T cells, glucose uptake was significantly inhibited by phloridzin (Fig. 4A,B).

Effect of JAK3 inhibitors on glucose uptake in murine CTLs

Additional experiments explored whether JAK3 regulates glucose uptake in CTLs. To this end, CTLs were treated with different JAK3 inhibitors and 2-NBD-glucose uptake determined (Fig. 4C,D). A 12 h incubation with the JAK3 inhibitors WHI-P131/JANEX-1 (4-(4′-Hydroxyphenyl)amino-6,7-dimethoxyquinazoline, 156 μM), JAK3 Inhibitor VI (0.5 μM) or WHI-P154 (4-[(3′-Bromo-4′-hydroxyphenyl)amino]-6,7-dimethoxyquinazoline, 11.2 μM) each resulted in significant reduction in 2-NBD-glucose uptake in CTLs (Fig. 4C,D), pointing to JAK3 sensitive regulation of SGLT1 activity.

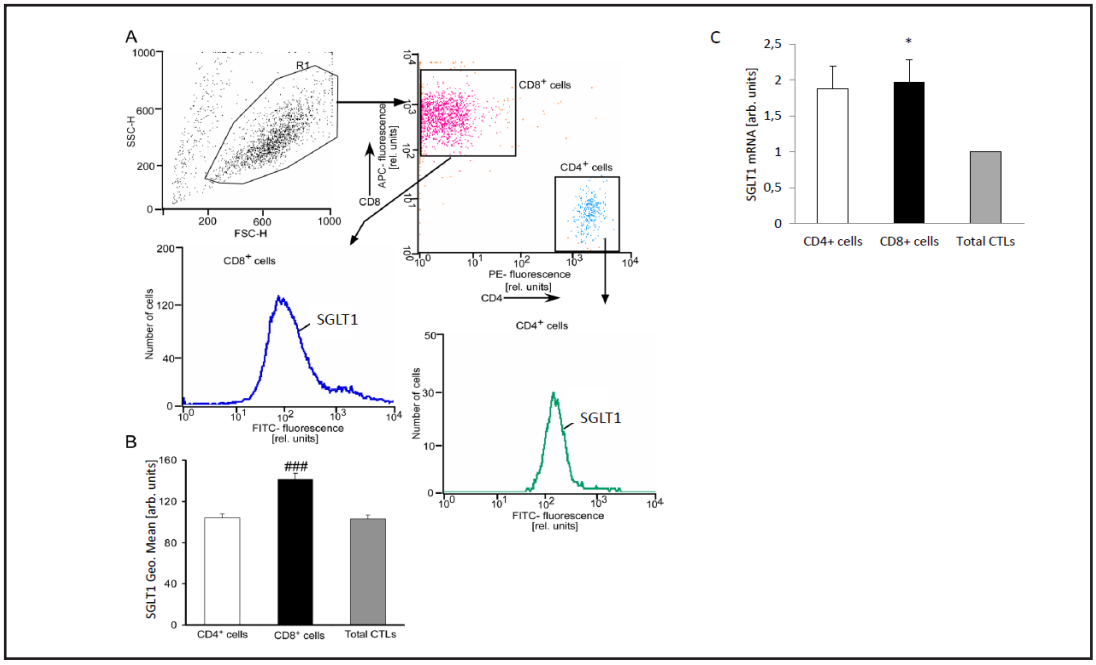

Fig. 3. Expression of SGLT1 in CD8⁺ and CD4⁺ subtype of activated murine cytotoxic T lymphocytes. CTLs were stained with primary murine anti-SGLT1 antibody followed by staining with secondary anti-rabbit FITC conjugated antibody. In addition cells were stained with PE-conjugated anti-CD4 antibody and APC-conjugated anti-CD8 antibody. The fluorescence was measured by standard multicolor flow cytometry settings. PE fluorescence measured in FL-2 and APC fluorescence measured in FL-4 channel together with FITC fluorescence measured in channel FL-1 on a FACS calibur (BD, Heidelberg, Germany). A: Gating of total CTL culture for CD8⁺ and CD4⁺ subtype of cells and original histograms for SGLT1 stain in CD8⁺ and CD4⁺ subtype of cells. Please do note the different scales in the histograms, as the number of CD8⁺ cells was higher than the number of CD4⁺ cells. B: Arithmetic means ± SEM (n = 4) of geometric mean for SGLT1 staining in CD8⁺ (black bar) and CD4⁺ (white bar) subtype of cells together with total CTL cells (grey bar) . ### ($p<0.001$) indicates statistically significant difference from the CD4⁺ subtype of cells as well as from total CTLs. C: Arithmetic means ± SEM (n = 4) of geometric mean for SGLT1 mRNA expression in CD8⁺ (black bar) and CD4⁺ (white bar) subtype of cells together with total CTL cells (grey bar) . * ($p<0.05$) indicates statistically significant difference from the CD8⁺ cells from total CTLs.

JAK3 inhibitors are known to inhibit proliferation of CTLs and induce apoptosis in CTLs and tumors over-expressing JAK3 [9, 72]. Forward scatter was thus determined in parallel to possibly detect induction of apoptosis. In preliminary experiments CTLs were thus incubated for several time points with Jak3 inhibitors. As a result, significant reduction in cell size was observed at exposure periods ≥16 hour (data not shown). Thus, a 12 hour incubation was chosen and up to this time point forward scatter remained constant (data not shown).

Similar to what has been observed for the total CTL population, the JAK3 inhibitors significantly reduced glucose uptake in both, CD4⁺ and CD8⁺ subtypes of CTLs (Fig. 5).

Expression of SGLT1 in Jurkat T cells and regulation of glucose uptake by SGLT1 inhibitor phloridzin

Further studies tested, whether SGLT1 is similarly expressed in the human T cell leukemia Jurkat T cell line [73]. SGLT1 expression in Jurkat T cells was detected with immunofluorescence and confocal microscopy. As shown in Fig.6A Jurkat T cells express SGLT1 protein, which is mainly localized in the cell membrane. Caco2 cells, used as positive control, similarly expressed SGLT1 in the cell membrane (Fig. 6A lower lane). The control staining with secondary antibody alone did not result in any significant fluorescence signal (Fig. 6A lower lane).

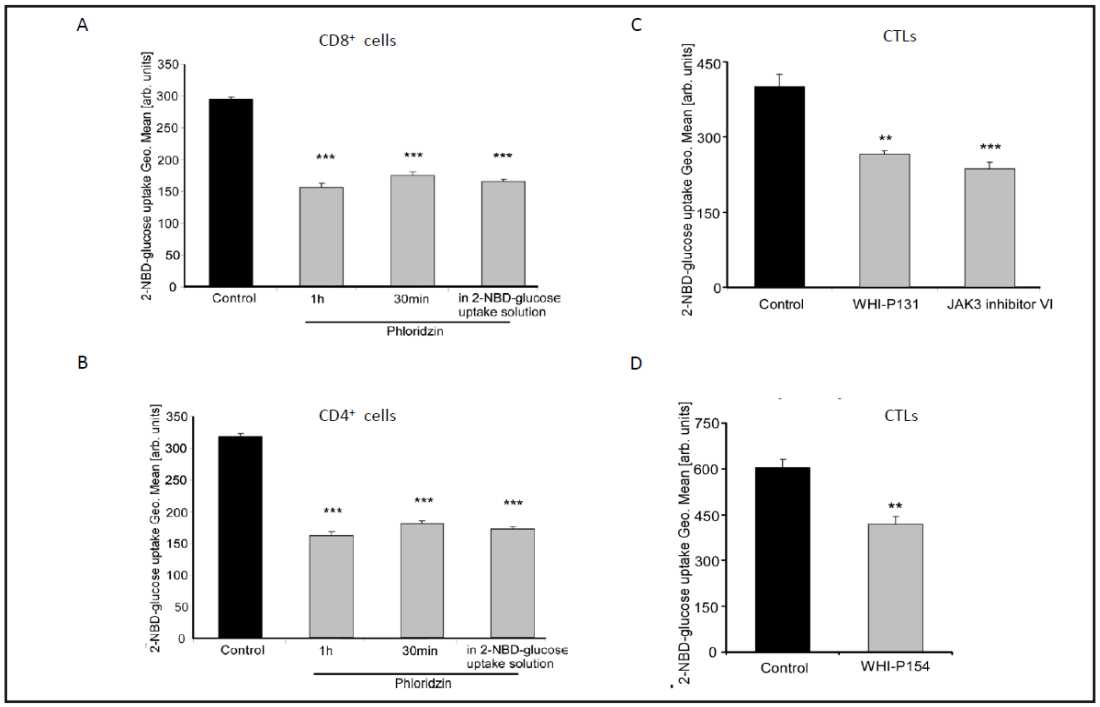

Fig. 4. Phloridzin and JAK3 inhibitor sensitive glucose uptake in $CD8^+$ and $CD4^+$ subtypes of activated murine cytotoxic T lymphocytes. A: Arithmetic means ± SEM (n = 4) of geometric means for the 2-NBD- glucose uptake into $CD8^+$ cells in the absence (black bar) and presence (grey bars) of phloridzin (0.2 mM) added for 1 hour. *** ($p<0.001$) indicates statistically significant difference from the absence of phloridzin in 2-NBD-glucose uptake. B: Arithmetic means ± SEM (n = 4) of geometric means for the 2-NBD- glucose uptake into $CD4^+$ cells in the absence (black bar) and presence (grey bars) of phloridzin (0.2 mM) added for 1 hour. *** ($p<0.001$) indicates statistically significant difference from the absence of phloridzin in 2-NBD-glucose uptake. C: Arithmetic means ± SEM (n = 4) of geometric means for the 2-NBD-glucose uptake into murine CTLs without (black bar) or with 12 hours incubation with JAK3 inhibitor 1 WHI-P131/JANEX-1 (4-(4′-Hydroxyphenyl)amino-6,7-dimethoxyquinazoline, 156 µM) or with JAK3 Inhibitor VI (0.5 µM) (grey bars) added 12 h prior to the experiment. **($p<0.01$), ***($p<0.001$) indicates statistically significant difference from the absence of JAK3 inhibitors. D: Arithmetic means ± SEM (n = 4) of geometric means for the 2-NBD-glucose uptake into murine CTLs in the absence (black bar) or presence of JAK3 inhibitor WHI-P154 (4-[(3′-Bromo-4′-hydroxyphenyl)amino]-6,7-dimethoxyquinazoline, 11.2 µM) (grey bar) added 12 h prior to the experiment. ** ($p<0.01$) indicates statistically significant difference from the absence of JAK3 inhibitors.

SGLT1 expression was also analysed by FACS analysis. FACS histograms of Jurkat T cells stained with primary and secondary antibody revealed a staining, which was one order of magnitude larger than the staining obtained with secondary antibody alone (Fig. 6B). SGLT1 was also detected by Western blotting in Jurkat T cells (Fig. 6C). A band of similar size and density was obtained in Caco2 cells as positive control. Hence, SGLT1 is expressed in Jurkat T cells.

Again, 2-NBD-glucose uptake was determined to estimate phloridzin sensitive glucose uptake into Jurkat T cells. As shown in Fig. 6D, incubation with phloridzin for 1h significantly decreased 2-NBD-glucose uptake into Jurkat T cells (Fig. 6E). Thus, similar to murine CTLs human Jurkat T cells express functional, phoridzin sensitive SGLT1 which marks its functional relevance in human T-cell leukemia.

Effect of JAK3 inhibitors on glucose uptake in Jurkat T cells

Similar to what has been shown in CTLs, glucose uptake by Jurkat T cells was influenced by JAK3 inhibitors. A 12 hours incubation with JAK3 inhibitor I WHI-P131/

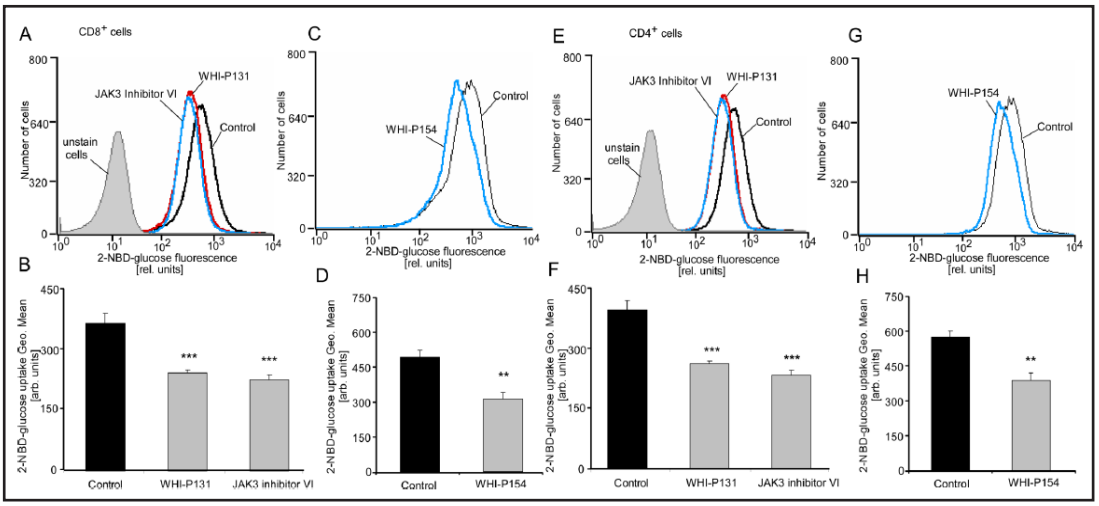

Fig. 5. Influence of JAK3 inhibitors on glucose uptake into CD8⁺ and CD4⁺ subtypes of activated murine cytotoxic T lymphocytes. A: Original histograms of 2-NBD-glucose uptake in CD8⁺ cells without (black line) or with 12 hours incubation with JAK3 inhibitor 1 WHI-P131/JANEX-1 (4-(4′-Hydroxyphenyl)amino-6,7-dimethoxyquinazoline, 156 µM) (red line) or with JAK3 Inhibitor VI (0.5 µM) (blue line). Grey filled histogram shows unstained cells. B: Arithmetic means ± SEM (n = 4) of geometric means for the 2-NBD-glucose uptake into murine CD8⁺ cells in the absence (black bar) or presence of JAK3 inhibitor WHI-P131 or JAK3 inhibitor VI (grey bars) added 12 h prior to the experiment. ***(p<0.001) indicates statistically significant difference from the absence of JAK3 inhibitors. C: Original histograms of 2-NBD-glucose uptake in CD8⁺ cells without (black line) or with incubation with JAK3 inhibitor WHI-P154 (4-[(3′-Bromo-4′-hydroxyphenyl)amino]-6,7-dimethoxyquinazoline, 11.2 µM) added 12 hours prior to the experiment (blue line). D: Arithmetic means ± SEM (n = 4) of geometric means for the 2-NBD-glucose uptake into murine CD8⁺ cells in the absence (black bar) or presence of JAK3 inhibitor WHI-P154 (grey bar) added 12 h prior to the experiment. ** (p<0.01) indicates statistically significant difference from the absence of JAK3 inhibitors. E: Original histograms of 2-NBD-glucose uptake in CD4⁺ cells without (black line) or with 12 hours incubation with JAK3 inhibitor 1 WHI-P131/JANEX-1 (4-(4′-Hydroxyphenyl)amino-6,7-dimethoxyquinazoline, 156 µM) (Red line) or with JAK3 Inhibitor VI (0.5 µM) (blue line). Grey filled histogram shows unstained cells. F: Arithmetic means ± SEM (n = 4) of geometric means for the 2-NBD-glucose uptake into murine CD4⁺ cells in the absence (black bar) or presence of JAK3 inhibitors WHI-P131 or JAK3 Inhibitor VI (grey bars) added 12 h prior to the experiment. ***(p<0.001) indicates statistically significant difference from the absence of JAK3 inhibitors. G: Original histograms of 2-NBD-glucose uptake in CD4⁺ cells without (black line) or with incubation with JAK3 inhibitor WHI-P154 (4-[(3′-Bromo-4′-hydroxyphenyl)amino]-6,7-dimethoxyquinazoline, 11.2 µM) added 12 hours prior to the experiment (blue line). H: Arithmetic means ± SEM (n = 4) of geometric means for the 2-NBD-glucose uptake into murine CD4⁺ cells in the absence (black bar) or presence of JAK3 inhibitor WHI-P154 (grey bar) added 12 h prior to the experiment. ** (p<0.01) indicates statistically significant difference from the absence of JAK3 inhibitors. Please do note the different scales in B and D as well as in F and H.

JANEX-1 (4-(4′-Hydroxyphenyl)amino-6,7-dimethoxyquinazoline, 156 µM), JAK3 Inhibitor VI (0.5 µM) or JAK3 inhibitor II WHI-P154 (4-[(3′-Bromo-4′-hydroxyphenyl)amino]-6,7-dimethoxyquinazoline, 11.2 µM) each resulted in a significant reduction in 2-NBD-glucose uptake into Jurkat T cells (Fig. 7A,B). Again, within the exposure time, forward scatter remained virtually constant and thus, there was no significant effect of the inhibitors on cell size (Fig. 7C).

JAK3 expression stimulated SGLT1 activity in Xenopus oocytes, an effect mimicked by active mutant ^{A568V}JAK3 but not by inactive ^{K851A}JAK3

In order to explore more directly whether JAK3 influences the function of SGLT1, the carrier was expressed in *Xenopus* oocytes with or without JAK3 and glucose induced inward

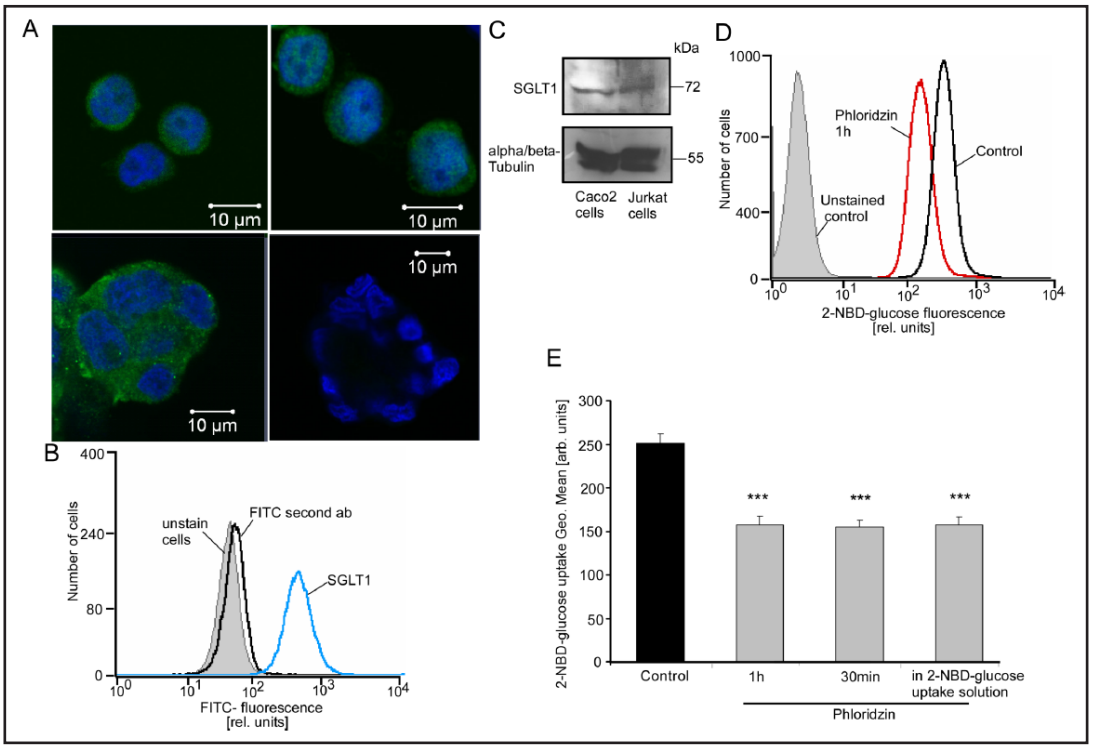

Fig. 6. SGLT1 expression and phloridzin sensitive glucose uptake in Jurkat T cells. A: Confocal microscopy of SGLT1 protein expression in Jurkat T cells (upper panels) and colon carcinoma (Caco2) cells (lower panels). The cells were subjected to immunofluorescent staining using rabbit anti-human SGLT1 antibody visualized by staining with anti-rabbit FITC-conjugated secondary antibody (green). DRAQ-5 dye (blue) was used for nuclear staining. Lower panel right picture shows Caco2 cells stained with only secondary antibody and DRAQ-5. B: Original histograms of the SGLT1 staining in Jurkat T cells. Histograms represent unstained cells (grey filled), cells stained with secondary FITC antibody only (black line) and cells stained with SGLT1 antibody followed by secondary antibody (blue line). C: Original Western blots showing expression of SGLT1 in Jurkat T cells and Caco2 cells. D: Original histograms of 2-NBD-glucose uptake in Jurkat T cells without (black line) or with 1 hour incubation with phloridzin (red line). Grey filled histogram shows unstained cells. E: Arithmetic means ± SEM (n = 4) of geometric means for the 2-NBD- glucose uptake into Jurkat T cells in the absence (black bar) and presence (grey bars) of phloridzin (0.2 mM) added for the indicated time periods. *** ($p<0.001$) indicates statistically significant difference from the absence of phloridzin in 2-NBD-glucose uptake.

current was taken as measure of glucose transport. In non-injected or water-injected *Xenopus* oocytes, glucose (10 mM) added to extracellular fluid did not induce an appreciable inward current. Thus, *Xenopus* oocytes do not express appreciable endogenous electrogenic glucose transport (Fig. 8). Glucose-induced current was similarly low in *Xenopus* oocytes expressing wild type JAK3 alone (Fig. 8A,B). In contrast, glucose (10 mM) induced a strong inward current (I_g) in *Xenopus* oocytes expressing SGLT1 (SLC5A1). The current was generated by electrogenic entry of Na^+ driving glucose transport. Expression of JAK3 in addition to SGLT1 significantly enhanced I_g (Fig. 8A,B).

According to kinetic analysis of the glucose-induced currents in SGLT1-expressing *Xenopus* oocytes (Fig. 8C) the maximal current was significantly higher (95 ± 6 nA, n = 3) in *Xenopus* oocytes expressing SGLT1 and JAK3 than in *Xenopus* oocytes expressing SGLT1 alone (64 ± 5 nA, n = 3). The glucose concentration required for half-maximal current (K_M) was similar in *Xenopus* oocytes expressing SGLT1 and JAK3 (891 ± 210 µM, n = 3) and in *Xenopus* oocytes expressing SGLT1 alone (795 ± 196 µM, n = 3). Thus, coexpression of JAK3 enhanced SGLT1 activity at least in part by increasing the maximal current.

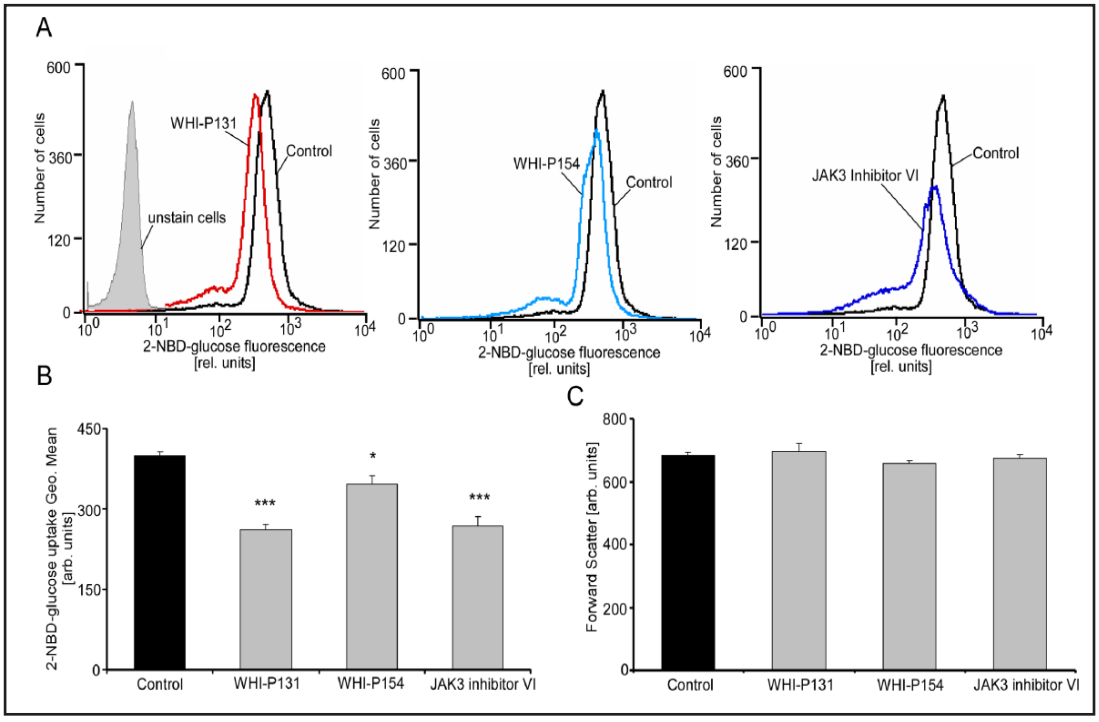

Fig. 7. Influence of JAK3 inhibitors on glucose uptake into Jurkat T cells. A: Original histograms of 2-NBD-glucose uptake in Jurkat T cells without (black line) or with 12 hours incubation with JAK3 inhibitors 1 WHI-P131/JANEX-1 (4-(4′-Hydroxyphenyl)amino-6,7-dimethoxyquinazoline, 156 μM) (red line), WHI-P154 (4-[(3′-Bromo-4′-hydroxyphenyl)amino]-6,7-dimethoxyquinazoline, 11.2 μM) (sky blue line) or JAK3 Inhibitor VI (0.5 μM) (dark blue line). Grey filled histogram shows unstained cells. B: Arithmetic means ± SEM (n = 6) of geometric means for the 2-NBD-glucose uptake into Jurkat T cells in the absence (black bar) or presence of JAK3 inhibitors WHI-P131, WHI-P154 or JAK3 Inhibitor VI (grey bars) added 12 h prior to the experiment. *($p<0.05$), ***($p<0.001$) indicates statistically significant difference from the absence of JAK3 inhibitors. C: Arithmetic means ± SEM (n = 6) of geometric means of forward scatter reflecting cell size of Jurkat T cells in the absence (black bar) or presence of JAK3 inhibitors WHI-P131/JANEX-1 or WHI-P154 or JAK3 Inhibitor VI (grey bars) added 12 h prior to the experiment.

The effect of JAK3 coexpression was mimicked by coexpression of the active mutant ^{A568V}JAK3 but not by the inactive mutant ^{K851A}JAK3 (Fig. 8A,B). The effect of ^{A568V}JAK3 tended to be higher than the effect of wild type JAK3, an effect, however, not reaching statistical significance.

Pharmacological JAK3 inhibition reversed the effect of JAK3 expression on SGLT1 activity in Xenopus oocytes

In *Xenopus* oocytes expressing SGLT1 and JAK3, preincubation of the oocytes with the JAK3 inhibitor WHI-P154 (4-[(3′-Bromo-4′-hydroxyphenyl)amino]-6,7-dimethoxyquinazoline, 11.2 μM) was followed by a significant decrease of I_g (Fig. 9A,B). The effect of the inhibitor was slow and was not apparent within 30 minutes. The effect reached statistical significance within 6 hours of preincubation of the inhibitors (Fig. 9B).

Effect of JAK3 and ^{A568V}JAK3 on SGLT1 protein abundance in Xenopus oocytes

The up-regulation of SGLT1 activity following coexpression of JAK3 could have resulted from increased carrier protein abundance in the plasma membrane. To explore that possibility, chemiluminescence was employed. As shown in Fig. 10A, the coexpression of JAK3 and ^{A568V}JAK3 was followed by a significant increase of SGLT1 protein abundance within the oocyte cell membrane.

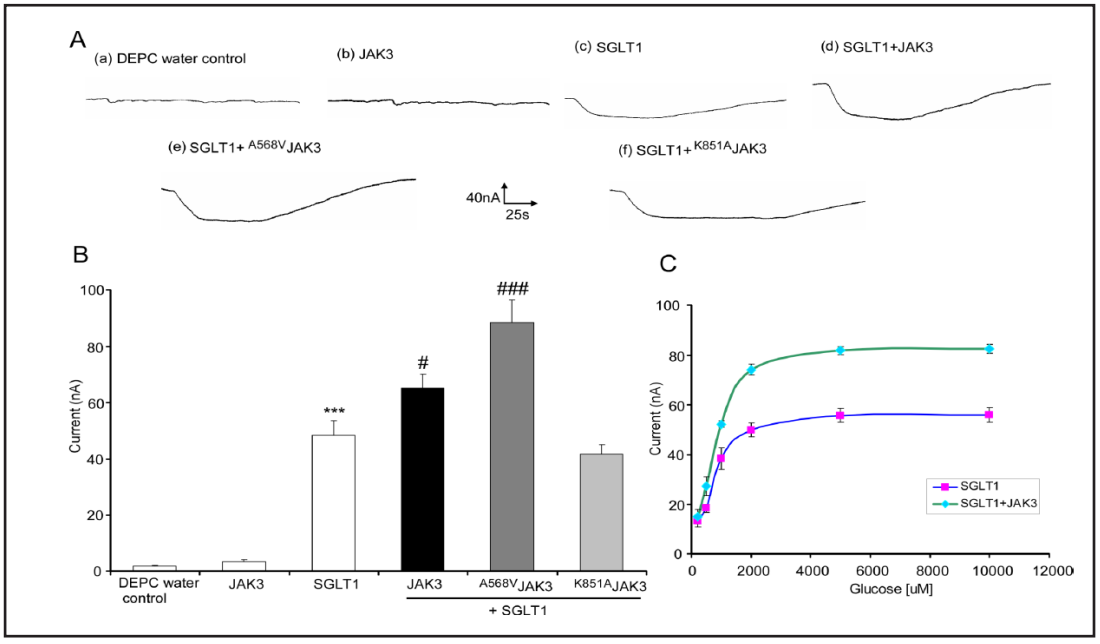

Fig. 8. Upregulation of electrogenic glucose transport in SGLT1-expressing *Xenopus* oocytes by wild type JAK3, by ^{A568V}JAK3 but not by ^{K851A}JAK3. A: Representative original tracings showing glucose (10 mM)-induced current (I_g) in *Xenopus* oocytes injected with water (a) and expressing JAK3 alone (b) or SGLT1 without (c) or with additional coexpression of wild type JAK3 (d) or ^{A568V}JAK3 (e), or inactive mutant ^{K851A}JAK3 (f). B: Arithmetic means ± SEM (n = 10-15) of glucose (10 mM)-induced current (I_g) in *Xenopus* oocytes injected with water (H_2O), expressing JAK3 alone (JAK3), or expressing SGLT1 without (SGLT1) or with additional coexpression of wild type JAK3 (SGLT1+JAK3) or SGLT1+^{A568V}JAK3 or SGLT1+^{K851A}JAK3. ***(p<0.001) indicates statistically significant difference from the absence of SGLT1. #(p<0.05), ### (p<0.001) indicates statistically significant difference from SGLT1 injected alone. C: Arithmetic means ± SEM (n = 3) of glucose induced current (I_g) as a function of glucose concentration in *Xenopus* oocytes expressing SLC5A1 (SGLT1) without and with JAK3.

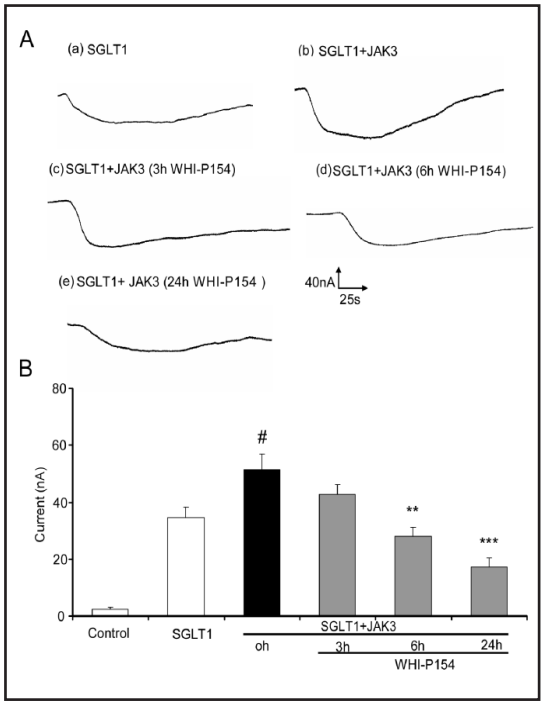

Fig. 9. Downregulation of electrogenic glucose transport in SGLT1+JAK3 expressing *Xenopus* oocytes by pharmacologic JAK3 inhibition. A: Representative original tracings showing glucose (10 mM)-induced current (I_g) in *Xenopus* oocytes injected with (left panel) SGLT1 alone (a), or coexpressing SGLT1 with JAK3 without (b), or with a 3 hour (c) or 6 hour (d) or 24 hour (e) pretreatment with JAK3 inhibitor WHI-P154 (4-[(3′-Bromo-4′-hydroxyphenyl) amino]-6,7-dimethoxyquinazoline, 11.2 μM). B: Arithmetic means ± SEM (n = 6-8) of glucose (10 mM)-induced current (I_g) in *Xenopus* oocytes injected with SGLT1 without (SGLT1) or with (SGLT1+JAK3) additional coexpression of wild type JAK3 in the absence of inhibitor (0 h) or following a 3 h, 6 h, or 24 h pretreatment with WHI-P154 (4-[(3′-Bromo-4′-hydroxyphenyl)amino]-6,7-dimethoxyquinazoline, 11.2 μM), #(p<0.05) indicates statistically significant difference from SGLT1 injected alone (absence of JAK3). **(p<0.01), ***(p<0.001) indicates statistically significant difference from the absence of JAK3 inhibitors (SGLT1+JAK3).

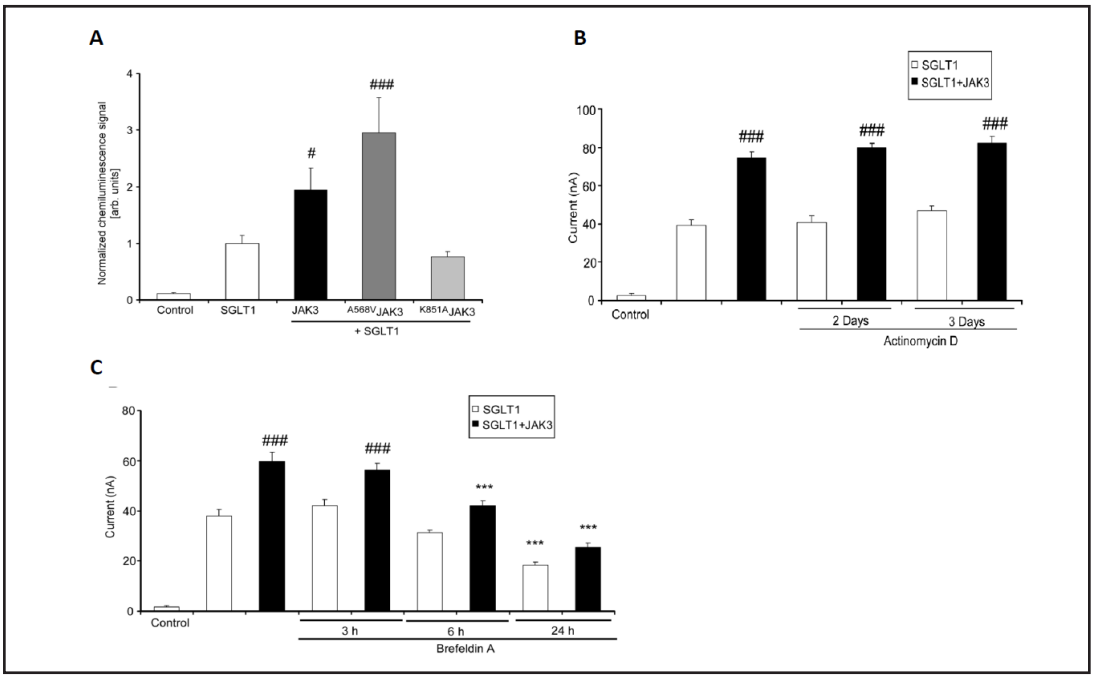

Fig. 10. Upregulation of surface SGLT1 protein abundance in SGLT1-expressing *Xenopus* oocytes by co-expression of JAK3 and ^{A568V}JAK3 and effects of actinomycin D and brefeldin A on electrogenic glucose transport. A: Arithmetic means ± SEM (n = 24-39) of the normalized chemiluminescence reflecting SGLT1 protein abundance in *Xenopus* oocytes injected with SGLT1 alone (SGLT1), or expressing SGLT1 with ^{A568V}-JAK3 (SGLT1+^{A568V}JAK3). #(p<0.05), ###(p<0.001) indicates statistically significant difference from SGLT1 injected alone. B: Arithmetic means ± SEM (n = 4-7) of glucose (10 mM)-induced current (I_g) in *Xenopus* oocytes injected with SGLT1 without (white bars) and with JAK3 (black bars) in the presence and absence of 10 μM actinomycin D 2-3 days prior to the measurement. ###(p<0.001) indicates statistically significant difference from SGLT1 injected alone. C: Arithmetic means ± SEM (n = 12-16) of glucose (10 mM)-induced current (I_g) in *Xenopus* oocytes injected with SGLT1 without (white bars) and with (black bars) JAK3 in the presence and absence of 5 μM brefeldin A for 0-24 hours prior to the measurement. ###(p<0.001) indicates statistically significant difference from SGLT1 injected alone, ***(p<0.001) indicates significant difference from the absence of brefeldin A.

Effect of brefeldin A and actinomycin D on glucose transport in SGLT1+JAK3 expressing Xenopus oocytes

JAK3 could have enhanced SGLT1 by influencing transcription of a posttranscriptional regulator of SGLT1. Thus, in additional experiments SGLT1+JAK3 expressing oocytes were incubated 2-3 days with and without actinomycin D (10 μM), an inhibitor of transcription. As a result, actinomycin D did not significantly modify I_g in *Xenopus* oocytes coexpressing JAK3 and SGLT1 (Fig. 10B).

The increased SGLT1 protein abundance in the cell membrane of SGLT1 expressing oocytes following coexpression of JAK3 could have resulted from either accelerated insertion of new carriers into or slowed clearance of carriers from the cell membrane. For discrimination between those two possibilities SGLT1-expressing *Xenopus* oocytes were treated with 5 μM brefeldin A, which blocks the insertion of new carrier protein into the cell membrane [74].

As shown in Fig. 10C, the glucose induced current declined in the presence of brefeldin A at a similar rate in SGLT1 and JAK3 expressing *Xenopus* oocytes and in oocytes expressing SGLT1 alone, an observation suggesting that JAK3 increases SGLT1 activity by stimulating carrier insertion into rather than by delaying the retrieval of carrier protein from the cell membrane.

Discussion

The present study shows for the first time expression of the high affinity Na^+ coupled glucose transporter SGLT1 in activated murine cytotoxic T cells and in human Jurkat T cells. The carrier accomplishes uphill transport of glucose driven by Na^+ entry down its electrochemical gradient. SGLT1 dependent cellular glucose uptake may be of prime significance for glucose uptake and function of CTL under glucose deprived conditions. At ample extracellular glucose concentration some 50% of glucose uptake is phloridzin sensitive and thus mediated by SGLT1. The residual uptake is presumably accomplished by GLUT1 [75], which mediates passive transport and is unable to operate against a chemical glucose gradient [76, 77]. At decreased extracellular glucose the contribution of SGLT1 to cellular glucose uptake is thus expectedly much higher. As soon as extracellular glucose concentration decreases to values lower than intracellular glucose concentration, cellular net glucose uptake fully depends on SGLT1, which, in contrast to glucose carriers of the GLUT family, is able to transport glucose against a glucose gradient [19].

Quiescent naive and memory $CD8^+$ T cells do require energy for survival and migration. Effector CTLs have a substantially higher energy demand because they need to proliferate rapidly and produce effector cytokines [36]. It is thus essential that upon activation, $CD8^+$ T cells increase cellular energy production and nutrient uptake to satisfy increased biosynthetic demands [42]. Following activation, CTLs upregulate amino acid transporters, the transferrin receptor and glucose transporters at the cell surface in response to extrinsic signals from antigens and cytokines [38, 75]. Inhibition of aerobic and anaerobic energy production in effector cells completely abolished cytotoxicity [78], an observation illustrating energy requirements for efficient cell-mediated cytotoxicity.

In resting T-cells, ATP is largely generated by breakdown of glucose, lipids and amino acids through oxidative phosphorylation, which yields large amounts of ATP [38]. In proliferating lymphocytes, lipid precursors and amino acids are, instead, shunted into the production of macromolecules that are required for anabolic cell growth. As a result, continued ATP production becomes progressively more dependent on the degradation of glucose by glycolysis [79]. Preferential ATP generation from glycolysis is maintained under both aerobic and anaerobic conditions [80, 81]. Thus, even in the presence of oxygen, proliferating lymphocytes generate ATP mainly by glycolysis [38, 82]. If glucose delivery and thus glycolytic flux are not sufficient, function and survival of lymphocytes is compromised and proapoptotic Bcl-2 family members become activated thus inducing cell death [42, 79]. Failure to up-regulate the metabolic machinery thus leads to anergic T cells [83].

As compared to oxidative phosphorylation glycolysis yields only a small fraction of ATP and sufficient ATP generation from glycolysis requires excessive glucose uptake and consumption [41]. In activated T cells, the switch from oxidative phosphorylation to aerobic glycolysis, i.e. oxygen-independent production of ATP from glucose, is thus paralleled by high-level glucose uptake, which has hitherto been considered to be accomplished by upregulation of expression and function of the glucose carrier GLUT1 (SLC2A1) [75]. The present data reveals that SGLT1 also plays a significant role in glucose uptake by CTLs. The function of this carrier may be particularly important for lymphocytes invading in tissues with low extracellular glucose concentrations due an imbalance of glucose delivery from blood and excessive cellular glucose utilization.

SGLT1 is mainly expressed in intestinal and renal tubular epithelia [19, 84]. SGLT1 is, however, in addition expressed in a variety of tumor cells [20-27]. Similar to activated lymphocytes [75, 85-87], tumor cells further express the facilitative glucose transporter GLUT1 [76, 77]. It is hypothesized that the facilitative glucose carrier cannot cover the excessive glucose demand of tumor cells under conditions of low extracellular glucose concentrations [22].

The employment of SGLT1 for cellular glucose uptake is a double edged sword, as unlike the passive GLUT carriers, Na^+-coupled glucose uptake requires ATP-consuming extrusion of the cotransported Na^+ by the Na^+/K^+ ATPase. Inability to extrude the cotransported Na^+ is expected

to result in cellular K^+ loss, followed by depolarization, Cl^- entry, cellular accumulation of NaCl with osmotically obliged water and thus cell swelling [88]. Since Na^+/K^+ ATPase extrudes 3 Na^+ ions for one ATP, the energy required for subsequent extrusion of cotransported Na^+ is, however, only a fraction of the energy gained by the degradation of glucose, even if glucose is utilized for ATP generation by glycolysis without oxidative metabolism.

The present observations also disclose JAK3 as a novel regulator of the high affinity Na^+ coupled glucose transporter SGLT1. The pharmacological evidence in CTLs and Jurkat T cells has been confirmed by results utilizing the *Xenopus* oocytes expression system. In *Xenopus laevis* oocytes, JAK3 up-regulates SGLT1 protein abundance in the cell membrane and thus increases the electrogenic cellular glucose uptake. Accordingly, co-expression of JAK3 increased the maximal current reflecting maximal glucose transport rate. The experiments with brefeldin A suggest that JAK3 influences the insertion of carrier protein into rather than delaying carrier retrieval from the cell membrane.

JAK3 could influence SGLT1 protein abundance in the cell membrane by direct phosphorylation of the carrier protein or by phosphorylation of other signaling molecules, which in turn up-regulate SGLT1. SGLT1 is regulated by JAK2 [18], protein kinase A (PKA) [89, 90], protein kinase C (PKC) [89, 90], serum- and glucocorticoid-inducible kinase [91] and AMP-activated kinase [92]. Similar to JAK3, those kinases modify SGLT1 activity by influencing the carrier protein abundance within the plasma membrane.

Genetic deficiency of JAK3 leads to abrogation of signal transduction through the common gamma chain (γc) and thus to immunodeficiency suggesting that specific inhibition of JAK3 may result in immunosuppression [93]. Unexpectedly, a JAK3-selective inhibitor was less efficient in abolishing STAT5 phosphorylation than pan-JAK inhibitors [15]. It has been shown that the two JAK isoforms involved in signaling through γc utilizing cytokine receptors are not equally important and that JAK1 plays a dominant role over JAK3 [15]. Hence, additional mechanisms and regulation by JAK3 in T cells may be responsible for immunodeficiency associated with Jak3 deficiency. Inhibition of glucose uptake in CTLs by JAK3 inhibitors may provide a further explanation for the immunosuppressive effect of JAK3 deficiency and apoptosis inducing effect of JAK3 inhibitors in T cells. Along those lines downregulation of glucose transport has previously been shown to be an early effector mechanism in CD95-induced apoptosis of activated human T cells [94].

In conclusion, SGLT1 is expressed in murine CTLs and human Jurkat T cells and contributes significantly to glucose uptake in those cells. JAK3 up-regulates the Na^+-coupled glucose transporter SGLT1 by increasing the carrier protein abundance in the cell membrane. This effect of JAK3 could contribute to cellular glucose delivery in CTLs.

Acknowledgements

The authors acknowledge the meticulous preparation of the manuscript by Lejla Subasic and Sari Rübe and technical support by Elfriede Faber. The study was supported by the Deutsche Forschungsgemeinschaft (GRK 1302, SFB 773 B4/A1, La 315/13-3) and Open Access Publishing Fund of Tuebingen University.

Disclosure Statement

The authors declare that there is no conflict of interest.

References

1 Cornejo MG, Boggon TJ, Mercher T: JAK3: a two-faced player in hematological disorders. Int. J Biochem Cell Biol 2009;41:2376-2379.
2 Ghoreschi K, Laurence A, O'Shea JJ: Janus kinases in immune cell signaling. Immunol Rev 2009;228:273-287.

3 Imada K, Leonard WJ: The Jak-STAT pathway. Mol Immunol 2000;37:1-11.
4 O'Shea JJ, Gadina M, Schreiber RD: Cytokine signaling in 2002: new surprises in the Jak/Stat pathway. Cell 2002;109:S121-S131.
5 Shuai K, Liu B: Regulation of JAK-STAT signalling in the immune system. Nat Rev Immunol 2003;3:900-911.
6 de Totero D, Meazza R, Capaia M, Fabbi M, Azzarone B, Balleari E, Gobbi M, Cutrona G, Ferrarini M, Ferrini S: The opposite effects of IL-15 and IL-21 on CLL B cells correlate with differential activation of the JAK/STAT and ERK1/2 pathways. Blood 2008;111:517-524.
7 Fainstein N, Vaknin I, Einstein O, Zisman P, Ben Sasson SZ, Baniyash M, Ben Hur T: Neural precursor cells inhibit multiple inflammatory signals. Mol Cell Neurosci 2008;39:335-341.
8 Nakayama J, Yamamoto M, Hayashi K, Satoh H, Bundo K, Kubo M, Goitsuka R, Farrar MA, Kitamura D: BLNK suppresses pre-B-cell leukemogenesis through inhibition of JAK3. Blood 2009;113:1483-1492.
9 Kim BH, Oh SR, Yin CH, Lee S, Kim EA, Kim MS, Sandoval C, Jayabose S, Bach EA, Lee HK, Baeg GH: MS-1020 is a novel small molecule that selectively inhibits JAK3 activity. Br J Haematol 2010;148:132-143.
10 Uckun FM, Vassilev A, Dibirdik I, Tibbles H: Targeting JAK3 tyrosine kinase-linked signal transduction pathways with rationally-designed inhibitors. Anticancer Agents Med Chem 2007;7:612-623.
11 Yamaoka K, Min B, Zhou YJ, Paul WE, O'Shea JJ: Jak3 negatively regulates dendritic-cell cytokine production and survival. Blood 2005;106:3227-3233.
12 Ananthakrishnan R, Hallam K, Li Q, Ramasamy R: JAK-STAT pathway in cardiac ischemic stress. Vascul Pharmacol 2005;43:353-356.
13 Nagel S, Papadakis M, Pfleger K, Grond-Ginsbach C, Buchan AM, Wagner S: Microarray analysis of the global gene expression profile following hypothermia and transient focal cerebral ischemia. Neuroscience 2012;208:109-122.
14 Wang G, Qian P, Jackson FR, Qian G, Wu G: Sequential activation of JAKs, STATs and xanthine dehydrogenase/oxidase by hypoxia in lung microvascular endothelial cells. Int. J Biochem Cell Biol 2008;40:461-470.
15 Haan C, Rolvering C, Raulf F, Kapp M, Druckes P, Thoma G, Behrmann I, Zerwes HG: Jak1 has a dominant role over Jak3 in signal transduction through gammac-containing cytokine receptors. Chem Biol 2011;18:314-323.
16 Malinge S, Ragu C, Della-Valle V, Pisani D, Constantinescu SN, Perez C, Villeval JL, Reinhardt D, Landman-Parker J, Michaux L, Dastugue N, Baruchel A, Vainchenker W, Bourquin JP, Penard-Lacronique V, Bernard OA: Activating mutations in human acute megakaryoblastic leukemia. Blood 2008;112:4220-4226.
17 Walters DK, Mercher T, Gu TL, O'Hare T, Tyner JW, Loriaux M, Goss VL, Lee KA, Eide CA, Wong MJ, Stoffregen EP, McGreevey L, Nardone J, Moore SA, Crispino J, Boggon TJ, Heinrich MC, Deininger MW, Polakiewicz RD, Gilliland DG, Druker BJ: Activating alleles of JAK3 in acute megakaryoblastic leukemia. Cancer Cell 2006;10:65-75.
18 Hosseinzadeh Z, Bhavsar SK, Shojaiefard M, Saxena A, Merches K, Sopjani M, Alesutan I, Lang F: Stimulation of the glucose carrier SGLT1 by JAK2. Biochem Biophys Res Commun 2011;408:208-213.
19 Wright EM, Turk E: The sodium/glucose cotransport family SLC5. Pflugers Arch 2004;447:510-518.
20 Casneuf VF, Fonteyne P, Van Damme N, Demetter P, Pauwels P, de Hemptinne B, De Vos M, Van de WC, Peeters M: Expression of SGLT1, Bcl-2 and p53 in primary pancreatic cancer related to survival. Cancer Invest 2008;26:852-859.
21 Engelman JA, Cantley LC: A sweet new role for EGFR in cancer. Cancer Cell 2008;13:375-376.
22 Ganapathy V, Thangaraju M, Prasad PD: Nutrient transporters in cancer: relevance to Warburg hypothesis and beyond. Pharmacol Ther 2009;121:29-40.
23 Ishikawa N, Oguri T, Isobe T, Fujitaka K, Kohno N: SGLT gene expression in primary lung cancers and their metastatic lesions. Jpn J Cancer Res 2001;92:874-879.
24 Kidd M, Modlin IM, Gustafsson BI, Drozdov I, Hauso O, Pfragner R: Luminal regulation of normal and neoplastic human EC cell serotonin release is mediated by bile salts, amines, tastants, and olfactants. Am. J Physiol Gastrointest. Liver Physiol 2008;295:G260-G272.
25 Macheda ML, Rogers S, Best JD: Molecular and cellular regulation of glucose transporter (GLUT) proteins in cancer. J Cell Physiol 2005;202:654-662.
26 Matosin-Matekalo M, Mesonero JE, Delezay O, Poiree JC, Ilundain AA, Brot-Laroche E: Thyroid hormone regulation of the Na+/glucose cotransporter SGLT1 in Caco-2 cells. Biochem J 1998;334:633-640.
27 Weihua Z, Tsan R, Huang WC, Wu Q, Chiu CH, Fidler IJ, Hung MC: Survival of cancer cells is maintained by EGFR independent of its kinase activity. Cancer Cell 2008;13:385-393.

28 Bauer DE, Harris MH, Plas DR, Lum JJ, Hammerman PS, Rathmell JC, Riley JL, Thompson CB: Cytokine stimulation of aerobic glycolysis in hematopoietic cells exceeds proliferative demand. FASEB J 2004;18:1303-1305.
29 Elstrom RL, Bauer DE, Buzzai M, Karnauskas R, Harris MH, Plas DR, Zhuang H, Cinalli RM, Alavi A, Rudin CM, Thompson CB: Akt stimulates aerobic glycolysis in cancer cells. Cancer Res 2004;64:3892-3899.
30 Charni S, de Bettignies G, Rathore MG, Aguilo JI, van den Elsen PJ, Haouzi D, Hipskind RA, Enriquez JA, Sanchez-Beato M, Pardo J, Anel A, Villalba M: Oxidative phosphorylation induces de novo expression of the MHC class I in tumor cells through the ERK5 pathway. J Immunol 2010;185:3498-3503.
31 Rose T, Pillet AH, Lavergne V, Tamarit B, Lenormand P, Rousselle JC, Namane A, Theze J: Interleukin-7 compartmentalizes its receptor signaling complex to initiate CD4 T lymphocyte response. J Biol Chem 2010;285:14898-14908.
32 Leiprecht N, Munoz C, Alesutan I, Siraskar G, Sopjani M, Foller M, Stubenrauch F, Iftner T, Lang F: Regulation of Na(+)-coupled glucose carrier SGLT1 by human papillomavirus 18 E6 protein. Biochem Biophys Res Commun 2011;404:695-700.
33 zur Hausen H: Papillomaviruses and cancer: from basic studies to clinical application. Nat Rev Cancer 2002;2:342-350.
34 Cogliano V, Baan R, Straif K, Grosse Y, Secretan B, El Ghissassi F: Carcinogenicity of human papillomaviruses. Lancet Oncol 2005;6:204.
35 Parkin DM, Bray F: Chapter 2: The burden of HPV-related cancers. Vaccine 2006;24 Suppl 3:S3/11-S13/25.
36 Finlay D, Cantrell DA: Metabolism, migration and memory in cytotoxic T cells. Nat Rev Immunol 2011;11:109-117.
37 Caldwell CC, Kojima H, Lukashev D, Armstrong J, Farber M, Apasov SG, Sitkovsky MV: Differential effects of physiologically relevant hypoxic conditions on T lymphocyte development and effector functions. J Immunol 2001;167:6140-6149.
38 Fox CJ, Hammerman PS, Thompson CB: Fuel feeds function: energy metabolism and the T-cell response. Nat Rev Immunol 2005;5:844-852.
39 Michalek RD, Gerriets VA, Jacobs SR, Macintyre AN, Maciver NJ, Mason EF, Sullivan SA, Nichols AG, Rathmell JC: Cutting edge: distinct glycolytic and lipid oxidative metabolic programs are essential for effector and regulatory CD4+ T cell subsets. J Immunol 2011;186:3299-3303.
40 Jacobs SR, Michalek RD, Rathmell JC: IL-7 is essential for homeostatic control of T cell metabolism in vivo. J Immunol 2010;184:3461-3469.
41 Vander Heiden MG, Cantley LC, Thompson CB: Understanding the Warburg effect: the metabolic requirements of cell proliferation. Science 2009;324:1029-1033.
42 Cham CM, Driessens G, O'Keefe JP, Gajewski TF: Glucose deprivation inhibits multiple key gene expression events and effector functions in CD8+ T cells. Eur J Immunol 2008;38:2438-2450.
43 Cham CM, Gajewski TF: Glucose availability regulates IFN-gamma production and p70S6 kinase activation in CD8+ effector T cells. J Immunol 2005;174:4670-4677.
44 Kojima H, Kobayashi A, Sakurai D, Kanno Y, Hase H, Takahashi R, Totsuka Y, Semenza GL, Sitkovsky MV, Kobata T: Differentiation stage-specific requirement in hypoxia-inducible factor-1alpha-regulated glycolytic pathway during murine B cell development in bone marrow. J Immunol 2010;184:154-163.
45 Dietl K, Renner K, Dettmer K, Timischl B, Eberhart K, Dorn C, Hellerbrand C, Kastenberger M, Kunz-Schughart LA, Oefner PJ, Andreesen R, Gottfried E, Kreutz MP: Lactic acid and acidification inhibit TNF secretion and glycolysis of human monocytes. J Immunol 2010;184:1200-1209.
46 Rodriguez-Prados JC, Traves PG, Cuenca J, Rico D, Aragones J, Martin-Sanz P, Cascante M, Bosca L: Substrate fate in activated macrophages: a comparison between innate, classic, and alternative activation. J Immunol 2010;185:605-614.
47 Roiniotis J, Dinh H, Masendycz P, Turner A, Elsegood CL, Scholz GM, Hamilton JA: Hypoxia prolongs monocyte/macrophage survival and enhanced glycolysis is associated with their maturation under aerobic conditions. J Immunol 2009;182:7974-7981.
48 Szabo I, Bock J, Jekle A, Soddemann M, Adams C, Lang F, Zoratti M, Gulbins E: A novel potassium channel in lymphocyte mitochondria. J Biol Chem 2005;280:12790-12798.
49 Gorboulev V, Schurmann A, Vallon V, Kipp H, Jaschke A, Klessen D, Friedrich A, Scherneck S, Rieg T, Cunard R, Veyhl-Wichmann M, Srinivasan A, Balen D, Breljak D, Rexhepaj R, Parker HE, Gribble FM, Reimann F, Lang F, Wiese S, Sabolic I, Sendtner M, Koepsell H: Na(+)-D-glucose cotransporter SGLT1 is pivotal for intestinal glucose absorption and glucose-dependent incretin secretion. Diabetes 2012;61:187-196.

50 Sinclair LV, Finlay D, Feijoo C, Cornish GH, Gray A, Ager A, Okkenhaug K, Hagenbeek TJ, Spits H, Cantrell DA: Phosphatidylinositol-3-OH kinase and nutrient-sensing mTOR pathways control T lymphocyte trafficking. Nat Immunol 2008;9:513-521.
51 Singh Y, Kaul V, Mehra A, Chatterjee S, Tousif S, Dwivedi VP, Suar M, Van Kaer L, Bishai WR, Das G: Mycobacterium tuberculosis controls microRNA-99b (miR-99b) expression in infected murine dendritic cells to modulate host immunity. J Biol Chem 2013;288:5056-5061.
52 Fezai M, Warsi J, Lang F: Regulation of the Na+,Cl- Coupled Creatine Transporter CreaT (SLC6A8) by the Janus Kinase JAK3. Neurosignals 2015;23:11-19.
53 Hosseinzadeh Z, Honisch S, Schmid E, Jilani K, Szteyn K, Bhavsar S, Singh Y, Palmada M, Umbach AT, Shumilina E, Lang F: The Role of Janus Kinase 3 in the Regulation of Na(+)/K(+) ATPase under Energy Depletion. Cell Physiol Biochem 2015;36:727-740.
54 Mohamed MR, Alesutan I, Foller M, Sopjani M, Bress A, Baur M, Salama RH, Bakr MS, Mohamed MA, Blin N, Lang F, Pfister M: Functional analysis of a novel I71N mutation in the GJB2 gene among Southern Egyptians causing autosomal recessive hearing loss. Cell Physiol Biochem 2010;26:959-966.
55 Warsi J, Abousaab A, Fezai M, Elvira B, Lang F: Regulation of Voltage Gated K+ Channel KCNE1/KCNQ1 by the Janus Kinase JAK3. Cell Physiol Biochem 2015;37:2476-2485.
56 Warsi J, Abousaab A, Lang F: Up-Regulation of Excitatory Amino Acid Transporters EAAT1 and EAAT2 by ss-Klotho. Neurosignals 2015;23:59-70.
57 Warsi J, Fezai M, Fores M, Elvira B, Lang F: Up-Regulation of Voltage Gated K+ Channels Kv1.3 and Kv1.5 by Protein Kinase PKB/Akt. Cell Physiol Biochem 2015;37:2454-2463.
58 Elvira B, Warsi J, Fezai M, Munoz C, Lang F: SPAK and OSR1 Sensitive Cell Membrane Protein Abundance and Activity of KCNQ1/E1 K+ Channels. Cell Physiol Biochem 2015;37:2032-2042.
59 Fezai M, Elvira B, Warsi J, Ben-Attia M, Hosseinzadeh Z, Lang F: Up-Regulation of Intestinal Phosphate Transporter NaPi-IIb (SLC34A2) by the Kinases SPAK and OSR1. Kidney Blood Press Res 2015;40:555-564.
60 Warsi J, Singh Y, Elvira B, Hosseinzadeh Z, Lang F: Regulation of Large Conductance Voltage-and Ca2+-Activated K+ Channels by the Janus Kinase JAK3. Cell Physiol Biochem 2015;37:297-305.
61 Ahmed M, Salker MS, Elvira B, Umbach AT, Fakhri H, Saeed AM, Shumilina E, Hosseinzadeh Z, Lang F: SPAK Sensitive Regulation of the Epithelial Na Channel ENaC. Kidney Blood Press Res 2015;40:335-343.
62 Elvira B, Munoz C, Borras J, Chen H, Warsi J, Ajay SS, Shumilina E, Lang F: SPAK and OSR1 dependent down-regulation of murine renal outer medullary K channel ROMK1. Kidney Blood Press Res 2014;39:353-360.
63 Warsi J, Dong L, Elvira B, Salker MS, Shumilina E, Hosseinzadeh Z, Lang F: SPAK dependent regulation of peptide transporters PEPT1 and PEPT2. Kidney Blood Press Res 2014;39:388-398.
64 Alesutan I, Voelkl J, Stockigt F, Mia S, Feger M, Primessnig U, Sopjani M, Munoz C, Borst O, Gawaz M, Pieske B, Metzler B, Heinzel F, Schrickel JW, Lang F: AMP-activated protein kinase alpha1 regulates cardiac gap junction protein connexin 43 and electrical remodeling following pressure overload. Cell Physiol Biochem 2015;35:406-418.
65 Almilaji A, Honisch S, Liu G, Elvira B, Ajay SS, Hosseinzadeh Z, Ahmed M, Munoz C, Sopjani M, Lang F: Regulation of the voltage gated K channel Kv1.3 by recombinant human klotho protein. Kidney Blood Press Res 2014;39:609-622.
66 Warsi J, Hosseinzadeh Z, Elvira B, Bissinger R, Shumilina E, Lang F: Regulation of ClC-2 activity by SPAK and OSR1. Kidney Blood Press Res 2014;39:378-387.
67 Almilaji A, Sopjani M, Elvira B, Borras J, Dermaku-Sopjani M, Munoz C, Warsi J, Lang UE, Lang F: Upregulation of the creatine transporter Slc6A8 by Klotho. Kidney Blood Press Res 2014;39:516-525.
68 Fezai M, Elvira B, Borras J, Ben-Attia M, Hoseinzadeh Z, Lang F: Negative regulation of the creatine transporter SLC6A8 by SPAK and OSR1. Kidney Blood Press Res 2014;39:546-554.
69 Munoz C, Pakladok T, Almilaji A, Elvira B, Decher N, Shumilina E, Lang F: Up-regulation of Kir2.1 (KCNJ2) by the serum & glucocorticoid inducible SGK3. Cell Physiol Biochem 2014;33:491-500.
70 Fezai M, Ahmed M, Hosseinzadeh Z, Elvira B, Lang F: SPAK and OSR1 Sensitive Kir2.1 K+ Channels. Neurosignals 2015;23:20-33.
71 Warsi J, Elvira B, Bissinger R, Shumilina E, Hosseinzadeh Z, Lang F: Downregulation of peptide transporters PEPT1 and PEPT2 by oxidative stress responsive kinase OSR1. Kidney Blood Press Res 2014;39:591-599.
72 Thompson JE, Cubbon RM, Cummings RT, Wicker LS, Frankshun R, Cunningham BR, Cameron PM, Meinke PT, Liverton N, Weng Y, DeMartino JA: Photochemical preparation of a pyridone containing tetracycle: a Jak protein kinase inhibitor. Bioorg. Med Chem Lett 2002;12:1219-1223.

73 Schneider U, Schwenk HU, Bornkamm G: Characterization of EBV-genome negative "null" and "T" cell lines derived from children with acute lymphoblastic leukemia and leukemic transformed non-Hodgkin lymphoma. Int J Cancer 1977;19:621-626.
74 Veyhl-Wichmann M, Friedrich A, Vernaleken A, Singh S, Kipp H, Gorboulev V, Keller T, Chintalapati C, Pipkorn R, Pastor-Anglada M, Groll J, Koepsell H: Phosphorylation of RS1 (RSC1A1) Steers Inhibition of Different Exocytotic Pathways for Glucose Transporter SGLT1 and Nucleoside Transporter CNT1, and an RS1-Derived Peptide Inhibits Glucose Absorption. Mol Pharmacol 2016;89:118-132.
75 Jacobs SR, Herman CE, Maciver NJ, Wofford JA, Wieman HL, Hammen JJ, Rathmell JC: Glucose uptake is limiting in T cell activation and requires CD28-mediated Akt-dependent and independent pathways. J Immunol 2008;180:4476-4486.
76 Mendez LE, Manci N, Cantuaria G, Gomez-Marin O, Penalver M, Braunschweiger P, Nadji M: Expression of glucose transporter-1 in cervical cancer and its precursors. Gynecol Oncol 2002;86:138-143.
77 Rudlowski C, Becker AJ, Schroder W, Rath W, Buttner R, Moser M: GLUT1 messenger RNA and protein induction relates to the malignant transformation of cervical cancer. Am J Clin. Pathol 2003;120:691-698.
78 Trinchieri G, De Marchi M: Antibody-dependent cell-mediated cytotoxicity in humans. II. Energy requirement. J Immunol 1975;115:256-260.
79 Maciver NJ, Jacobs SR, Wieman HL, Wofford JA, Coloff JL, Rathmell JC: Glucose metabolism in lymphocytes is a regulated process with significant effects on immune cell function and survival. J Leukoc Biol 2008;84:949-957.
80 Borregaard N, Herlin T: Energy metabolism of human neutrophils during phagocytosis. J Clin Invest 1982;70:550-557.
81 Sbarra AJ, Karnovsky ML: The biochemical basis of phagocytosis. I. Metabolic changes during the ingestion of particles by polymorphonuclear leukocytes. J Biol Chem 1959;234:1355-1362.
82 Frauwirth KA, Thompson CB: Regulation of T lymphocyte metabolism. J Immunol 2004;172:4661-4665.
83 Zheng Y, Delgoffe GM, Meyer CF, Chan W, Powell JD: Anergic T cells are metabolically anergic. J Immunol 2009;183:6095-6101.
84 Palazzo M, Gariboldi S, Zanobbio L, Selleri S, Dusio GF, Mauro V, Rossini A, Balsari A, Rumio C: Sodium-dependent glucose transporter-1 as a novel immunological player in the intestinal mucosa. J Immunol 2008;181:3126-3136.
85 Chakrabarti R, Jung CY, Lee TP, Liu H, Mookerjee BK: Changes in glucose transport and transporter isoforms during the activation of human peripheral blood lymphocytes by phytohemagglutinin. J Immunol 1994;152:2660-2668.
86 Jones KS, Akel S, Petrow-Sadowski C, Huang Y, Bertolette DC, Ruscetti FW: Induction of human T cell leukemia virus type I receptors on quiescent naive T lymphocytes by TGF-beta. J Immunol 2005;174:4262-4270.
87 Kuo CW, Mirsaliotis A, Brighty DW: Antibodies to the envelope glycoprotein of human T cell leukemia virus type 1 robustly activate cell-mediated cytotoxic responses and directly neutralize viral infectivity at multiple steps of the entry process. J Immunol 2011;187:361-371.
88 Lang F, Busch GL, Ritter M, Volkl H, Waldegger S, Gulbins E, Haussinger D: Functional significance of cell volume regulatory mechanisms. Physiol Rev 1998;78:247-306.
89 Hirsch JR, Loo DD, Wright EM: Regulation of Na+/glucose cotransporter expression by protein kinases in Xenopus laevis oocytes. J Biol. Chem 1996;271:14740-14746.
90 Subramanian S, Glitz P, Kipp H, Kinne RK, Castaneda F: Protein kinase-A affects sorting and conformation of the sodium-dependent glucose co-transporter SGLT1. J Cell Biochem 2009;106:444-452.
91 Dieter M, Palmada M, Rajamanickam J, Aydin A, Busjahn A, Boehmer C, Luft FC, Lang F: Regulation of glucose transporter SGLT1 by ubiquitin ligase Nedd4-2 and kinases SGK1, SGK3, and PKB. Obes Res 2004;12:862-870.
92 Sopjani M, Bhavsar SK, Fraser S, Kemp BE, Foller M, Lang F: Regulation of Na+-coupled glucose carrier SGLT1 by AMP-activated protein kinase. Mol Membr Biol 2010;27:137-144.
93 O'Shea JJ, Husa M, Li D, Hofmann SR, Watford W, Roberts JL, Buckley RH, Changelian P, Candotti F: Jak3 and the pathogenesis of severe combined immunodeficiency. Mol Immunol 2004;41:727-737.
94 Berridge MV, Tan AS, McCoy KD, Kansara M, Rudert F: CD95 (Fas/Apo-1)-induced apoptosis results in loss of glucose transporter function. J Immunol 1996;156:4092-4099.